

# Transcriptional Silencing of Nonsense Codon-Containing Immunoglobulin Minigenes

Marc Bühler,<sup>1,2</sup> Fabio Mohn,<sup>1</sup> Lukas Stalder,<sup>1</sup> and Oliver Mühlemann\*

<sup>1</sup>Institute of Cell Biology  
University of Bern  
Baltzerstrasse 4  
CH-3012 Bern  
Switzerland

## Summary

Cells possess mechanisms to prevent synthesis of potentially deleterious truncated proteins caused by premature translation-termination codons (PTCs). Here, we show that PTCs can induce silencing of transcription of its cognate gene. We demonstrate for immunoglobulin (Ig)- $\mu$  minigenes expressed in HeLa cells that this transcriptional silencing is PTC specific and reversible by treatment of the cells with histone deacetylase inhibitors. Furthermore, PTC-containing Ig- $\mu$  minigenes are significantly more associated with K9-methylated histone H3 and less associated with acetylated H3 than the PTC-free Ig- $\mu$  minigene. This nonsense-mediated transcriptional gene silencing (NMTGS) is also observed with an Ig- $\gamma$  minigene, but not with several classic NMD reporter genes, suggesting that NMTGS might be specific for Ig genes. NMTGS represents a nonsense surveillance mechanism by which truncation of a gene's open reading frame (ORF) induces transcriptional silencing through chromatin remodeling. Remarkably, NMTGS is inhibited by overexpression of the putative siRNase 3'hExo, suggesting that siRNA-like molecules are involved in NMTGS.

## Introduction

Aberrant mRNAs harboring premature translation-termination codons (hereafter called PTC<sup>+</sup> mRNAs) are dangerous for the cell, because they code for C-terminally truncated proteins that can function as dominant negative inhibitors over the full-length protein. PTC<sup>+</sup> mRNAs are recognized and selectively degraded by a translation-dependent posttranscriptional quality control system called nonsense-mediated mRNA decay (NMD) (Maquat, 2004; Mendell and Dietz, 2001; Singh and Lykke-Andersen, 2003; Wilusz et al., 2001). Although several proteins required for NMD were identified, and some of them are conserved between different species, the molecular mechanism of NMD is still not well understood and appears to differ between different eukaryotic species with regard to (1) the signals required for distinguishing a PTC from a physiological

stop codon and (2) the initiation of mRNA degradation (Gatfield and Izaurralde, 2004; Gatfield et al., 2003).

PTCs are generated in the genome by frameshift or nonsense mutations or by mutations that alter splicing signals of genes. Although the frequency of PTCs generated through these mechanisms is relatively low, T cell receptor (TCR) and Ig genes commonly acquire PTCs as a result of programmed V(D)J rearrangements during lymphocyte development (Li and Wilkinson, 1998). Because V(D)J recombination involves both loss of nucleotides and addition of nontemplated nucleotides at the junctions between recombined gene segments (Jung and Alt, 2004), two of three rearrangements are nonproductive, resulting in a frameshift that ultimately generates a PTC further downstream. Interestingly, steady-state PTC<sup>+</sup> transcript levels of TCR and Ig genes are reduced much more efficiently than PTC<sup>+</sup> mRNAs of the other genes that have been analyzed (Baumann et al., 1985; Bühler et al., 2004; Gudikote and Wilkinson, 2002). This apparently "super-efficient" NMD depends in TCR- $\beta$  and Ig- $\mu$  minigenes on the presence of the respective VDJ exon (Bühler et al., 2004; Gudikote and Wilkinson, 2002). PTC<sup>+</sup> TCR- $\beta$  and Ig- $\mu$  transcripts also differ from other PTC<sup>+</sup> mammalian mRNAs in that they do not comply with the so-called "50 nucleotides boundary rule" established for mammalian NMD (Nagy and Maquat, 1998), i.e., PTCs closer than 50 nucleotides to the 3'-most exon-exon junction still result in reduced mRNA levels (Baumann et al., 1985; Bühler et al., 2004; Carter et al., 1996; Wang et al., 2002).

In order to investigate the unusual effects caused by PTCs in Ig genes, we have constructed a mouse Ig- $\mu$  minigene and determined steady-state mRNA levels in HeLa cells of many constructs with PTCs at different positions (Bühler et al., 2004). In the course of these experiments, we performed nuclear run-on analysis with nuclei from polyclonal cell pools stably expressing the PTC-free or PTC<sup>+</sup> Ig- $\mu$  minigenes. Because all PTC-mediated effects reported so far are posttranscriptional, the run-on experiments were expected to show that the transcription rates of the different Ig- $\mu$  constructs did not differ from each other. However, in contrast to our expectation, we show here that transcription rates of PTC<sup>+</sup> Ig- $\mu$  constructs were reduced compared to PTC-free Ig- $\mu$  constructs and that this transcriptional silencing is accompanied by chromatin remodeling. Our data are reminiscent to the RNAi-mediated transcriptional silencing described in plants (Baulcombe, 2004; Matzke and Birchler, 2005), *S. pombe* (Hall et al., 2002; Volpe et al., 2002; Motamedi et al., 2004; Verdel et al., 2004), and *D. melanogaster* (Pal-Bhadra et al., 2004). Consistent with the idea that small double-stranded RNA molecules might also be involved in the nonsense-mediated transcriptional silencing of Ig- $\mu$  minigenes, we show that overexpression of 3'hExo, the human ortholog of the *C. elegans* siRNase ERI-1 (Kennedy et al., 2004), suppresses silencing of PTC<sup>+</sup> Ig- $\mu$ .

\*Correspondence: oliver.muehlemann@izb.unibe.ch

<sup>2</sup>Present address: Harvard Medical School, Department of Cell Biology, LHRB Room 517, 240 Longwood Avenue, Boston, Massachusetts 02115.

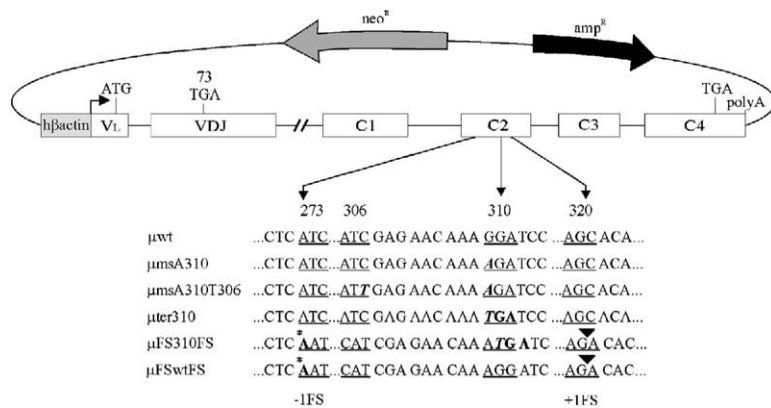


Figure 1. Schematic Representation of the Ig- $\mu$  Minigene Constructs

Mini $\mu$  constructs are under the control of the human  $\beta$ -actin promoter (light gray box). Exons are represented as white boxes, introns as lines. ATG and TGA indicate start and stop codons, respectively. Numbers depict amino acid positions of the nonsense, missense, or frameshift mutations. “ $\mu$ wt” denotes the PTC-free mini $\mu$  gene, PTC<sup>+</sup> constructs are named “ter” (for termination) followed by the amino acid position of the PTC. Missense mutations are named “ms” followed by the mutated nucleotide and the amino acid position. In constructs  $\mu$ FSter310FS and  $\mu$ FSwtFS, the reading frame between amino acid positions 273 and 320 was shifted by insertion of an A at position 273 (asterisk) and deletion of a C at position 320 (black triangle). Location and orientation of the neomycin and the ampicillin resistance genes are indicated by arrows.

## Results

### PTC-Specific Reduction of Ig- $\mu$ Transcription Rates

To examine in more detail the effects on mRNA and pre-mRNA caused by PTCs in Ig- $\mu$ , we have recently developed an Ig- $\mu$  minigene system (Buhler et al., 2004). This Ig- $\mu$  minigene (hereafter called mini $\mu$ ) is derived from the productively rearranged mouse Ig- $\mu$  gene expressed in the hybridoma cell line Sp6 (Ochi et al., 1983) and comprises the first six exons ( $V_{\text{leader}}$  exon to exon C4; Figure 1). Thus, the PTC-free wild-type construct (mini $\mu$ .wt) encodes the full-length, secreted form of the IgM heavy chain. To allow expression of the mini $\mu$  constructs in non-B cells, the constructs are driven by the human  $\beta$ -actin promoter. Besides measuring mini $\mu$  mRNA levels in transient transfection assays, we also transfected HeLa cells with mini $\mu$  constructs and selected polyclonal pools of cells that had integrated mini $\mu$  into the genome. Nuclei of these mini $\mu$ -expressing polyclonal cell pools were subsequently prepared to determine the Ig- $\mu$  transcription rates by nuclear run-on analysis. The <sup>32</sup>P-labeled nascent RNA was isolated and hybridized to single-stranded anti-sense mini $\mu$ .wt DNA, antisense glyceraldehyde phosphate dehydrogenase (GAPDH) cDNA, and pBluescript DNA immobilized on nylon filter strips.

Surprisingly, and in contrast to the current view that PTC<sup>+</sup> mRNA levels are downregulated exclusively post-transcriptionally, nuclear run-on analysis revealed that the transcription rate of PTC<sup>+</sup> mini $\mu$  constructs was reduced up to 12-fold compared to the PTC-free mini $\mu$ .wt (Figure 2A). Importantly, PTCs at two different positions within the coding region of Ig- $\mu$  led both to reduced transcription rates. In contrast, all tested mutations that do not generate a PTC, such as a missense mutation at amino acid 310 (mini $\mu$ .msA310), an additional missense mutation at amino acid position 306 (mini $\mu$ .msT306 msA310), a frameshift mutation that shifts the PTC at amino acid position 310 out of frame (mini $\mu$ .FS310FS), or the same frameshift mutation introduced into the mini $\mu$ .wt (mini $\mu$ .FSwtFS), did not alter the transcription rate significantly compared to mini $\mu$ .wt (Figure 2B).

These results strongly suggest that the transcriptional silencing of mini $\mu$  genes requires the presence of a premature translation-termination signal and that it is not an indirect consequence from disrupting a putative transcription-regulatory sequence element by the PTC-causing mutation. Therefore, we coined the term NMTGS to describe this nonsense codon-specific transcriptional silencing of our Ig- $\mu$  minigenes.

### NMTGS Is Accompanied by Deacetylation of Histone H3

Next, we wanted to know how the transcription rate of PTC<sup>+</sup> mini $\mu$  constructs was reduced. It is well established that the structure of the chromatin within a given gene is an important determinant for the transcriptional activity of this gene. Chromatin structure is modulated, at least in part, by enzymes that posttranslationally modify specific N-terminal amino acids on the histone proteins, and these modifications locally influence transcription activity (Fischle et al., 2003; Jenuwein and Allis, 2001). Although the pattern of the N-terminal histone modifications is complex, some specific modifications can be used as markers for transcriptionally active or silent chromatin, such as in histone H3 acetylation of K9 and K14 or methylation of K9, respectively (Dillon and Festenstein, 2002; Fischle et al., 2003; Jenuwein and Allis, 2001).

To investigate if NMTGS was accompanied by changes in chromatin structure, we performed chromatin immunoprecipitation (ChIP) assays. First, we immunoprecipitated genomic DNA fragments from HeLa cells expressing mini $\mu$ .wt or mini $\mu$ .ter310 by using an antibody raised against histone H3 that is acetylated at K9 and K14. The amount of mini $\mu$ -containing DNA in the immunoprecipitated material and in the cell lysate before immunoprecipitation (input) was determined relative to the amount of 18S rDNA in these samples by real-time PCR. The ratio between the relative amounts of immunoprecipitated mini $\mu$  and input mini $\mu$  is depicted in Figure 3A as “fold enrichment.” It shows that mini $\mu$ .wt is about 2.5- to 3-fold more associated with acetylated H3 than mini $\mu$ .ter310 (dark bars), indicating that NMTGS

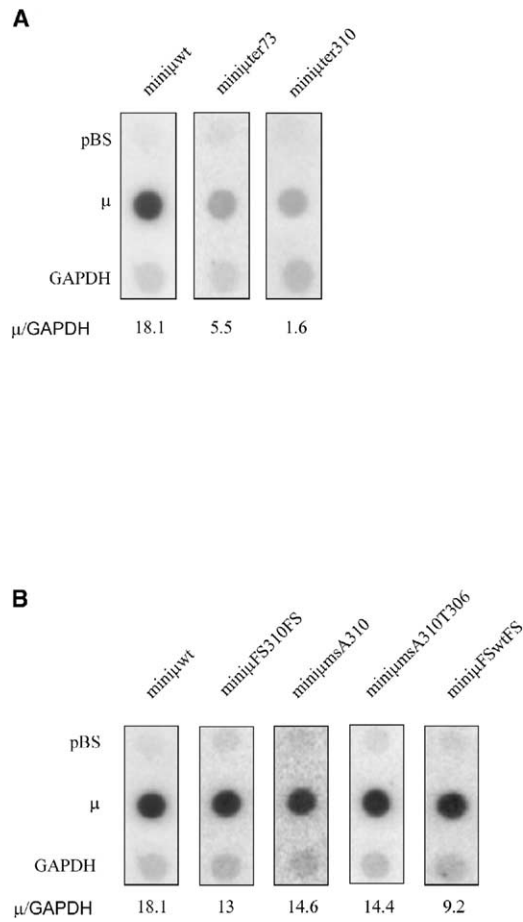


Figure 2. Nuclear Run-On Analysis with Nuclei of HeLa Cells Stably Expressing Various Mini $\mu$  Constructs Reveals PTC-Specific Reduction of Mini $\mu$  Transcription Rates

(A) Representative nuclear run-on assays with nuclei from polyclonal populations of HeLa cells stably expressing the indicated mini $\mu$  constructs.  $^{32}$ P-labeled nuclear RNA was isolated and hybridized to nylon filters containing the following single-stranded DNA probes: the empty pBluescript KS(-) vector (pBS) as a control for nonspecific hybridization, pBS containing the antisense mini $\mu$ wt sequence ( $\mu$ ), pBS containing the antisense sequence of the neomycin resistance gene (dots not shown, but quantified data is shown in Table S1), and pBS containing the antisense sequence of glyceraldehyde phosphate dehydrogenase (GAPDH). The number below each filter strip represents the quantified signal intensity for mini $\mu$ , normalized to the GAPDH signal ( $\mu$ /GAPDH).

(B) Nuclear run-on assays as in (A) were performed with nuclei from polyclonal cell pools stably expressing mini $\mu$  constructs with various mutations that do not generate a PTC (see Figure 1).

is associated with deacetylation of histone H3. By normalizing the amount of immunoprecipitated mini $\mu$  DNA to the amount of input mini $\mu$  DNA, we can rule out the possibility that the observed differences between the mini $\mu$ wt and the mini $\mu$ ter310-expressing cells could be due to different average plasmid copy numbers integrated into the two different cell pools. Theoretically, differences between the two polyclonal cell pools with regard to genomic integration loci of mini $\mu$  could be responsible for the differences observed in the ChIP assay. However, repetition of the experiment with inde-

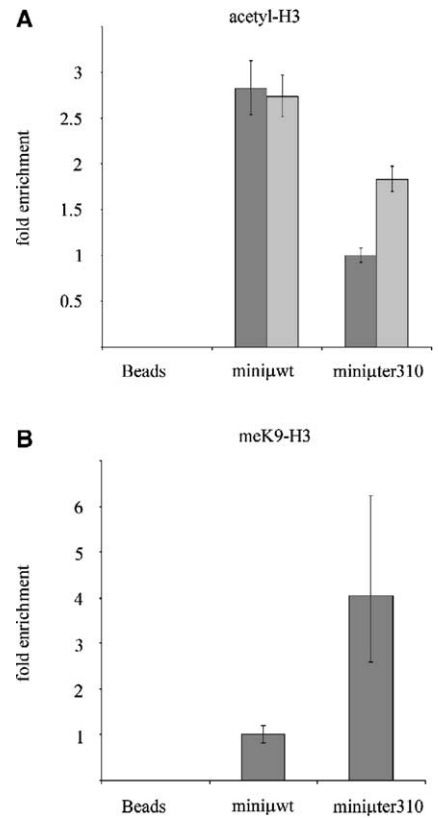


Figure 3. Transcriptional Gene Silencing of Mini $\mu$ ter310 Is Accompanied by Deacetylation of Histone H3 and K9 Methylation of H3

(A) Chromatin immunoprecipitation (ChIP) assay using an antibody to acetylated histone H3 as a marker for transcriptionally active chromatin. After formaldehyde crosslinking of cells expressing mini $\mu$ wt or mini $\mu$ ter310, sheared genomic DNA fragments were coprecipitated with an anti-acetyl-H3 antibody. The relative amount of mini $\mu$  DNA and 18S rDNA in the immunoprecipitated fraction and in the fraction before immunoprecipitation was quantified by real-time PCR. The relative mini $\mu$  DNA levels, normalized to 18S rDNA and to input levels, are represented as fold enrichment (dark gray bars; mini $\mu$ ter310 was set to 1). Light gray bars represent relative mini $\mu$  DNA levels coprecipitated from cells treated with 15 mM sodium butyrate for 24 hr before analysis.

(B) ChIP using an antibody to K9-methylated histone H3 as a marker for transcriptionally repressed chromatin. Genomic DNA fragments from the cells used in (A) were coprecipitated with a meK9-H3 antibody, and relative amounts of mini $\mu$  and endogenous  $\beta$ -globin DNA were quantified by real-time PCR. The relative mini $\mu$  DNA levels, double normalized to  $\beta$ -globin DNA and input, are represented as fold enrichment as in (A). Mini $\mu$ wt was set to 1.

In both panels, average values and SDs of three real-time PCR runs of one typical ChIP experiment are shown. Samples without antibody (Beads) served as a control for unspecific DNA precipitation.

pendent cell pools transfected with the same plasmids ruled out this explanation (Figure S1 available with this article online).

The acetylation state of histone N termini is determined by the balance of histone acetyltransferases (HATs) promoting hyperacetylation and transcriptional activity, and histone deacetylases (HDACs) promoting hypoacetylation and transcriptional silencing (Dillon and Festenstein, 2002; Fischle et al., 2003; Jenuwein

and Allis, 2001). We therefore tested if treatment of the cells with the potent HDAC inhibitor sodium butyrate (SB) prior to the ChIP assay increased the association of mini $\mu$ .ter310 with acetylated histone H3 (Figure 3A, light bars). Indeed, association of mini $\mu$ .ter310 with acetylated H3 increased 2-fold after SB treatment, almost reaching the level observed with mini $\mu$ .wt, whereas the amount of precipitated mini $\mu$ .wt did not change upon SB treatment. This suggests that mini $\mu$ .wt is already fully acetylated under normal conditions.

### NMTGS Is Accompanied by Lysine 9 Methylation of Histone H3

Although different histone modifications can induce a transcriptionally inactive state of chromatin, methylation of lysine 9 of histone H3 (meK9-H3) has been reported to highly correlate with repression of transcription (Litt et al., 2001; Nakayama et al., 2001; Noma et al., 2001). To test whether the transcriptionally silenced mini $\mu$ .ter310 associated with this specific histone modification, we performed the ChIP assay with a meK9-H3-specific antibody. The experiment was done as described above, except for using the endogenous  $\beta$ -globin gene for normalization, because the globin locus is assembled into transcriptionally silent heterochromatin in nonerythroid cells (Kim and Dean, 2004). We found that mini $\mu$ .ter310 is about 4-fold more associated with meK9-H3 than mini $\mu$ .wt (Figure 3B), which is consistent with its repressed transcription rate (Figure 2A).

In summary, ChIP analysis showed that PTC<sup>-</sup> and PTC<sup>+</sup> mini $\mu$  are preferentially associated with different posttranslational modifications of histone H3 and that NMTGS of mini $\mu$  is accompanied by deacetylation of K9 and K14 and by methylation of K9 in histone H3. The observation that the rate of neomycin transcription, the antibiotic resistance gene encoded on the mini $\mu$  expression plasmids, is also reduced about 3-fold in the mini $\mu$ .ter310-expressing cell line compared to cells expressing PTC-free mini $\mu$  (Table S1) further indicates that NMTGS results in formation of transcriptionally repressed chromatin around the integration site of PTC<sup>+</sup> mini $\mu$  genes.

### NMTGS Is Suppressed by Inhibition of Histone Deacetylases

Because treatment of the cells with the HDAC inhibitor SB increased the association of mini $\mu$ .ter310 with acetylated histone H3 in the ChIP assays (Figure 3A), we wondered whether this treatment also reversed the silenced transcription state. Indeed, nuclear run-on analysis performed with nuclei from mini $\mu$ .ter310-expressing cells prepared after treatment of the cells with SB for 24 hr showed an increased  $\mu$  transcription compared to the untreated nuclei (Figure 4A). Relative to transcription of GAPDH, transcription of mini $\mu$ .ter310 increased 8-fold, reaching a level similar to that measured with PTC-free mini $\mu$  constructs (Figure 2). Thus, the SB treatment almost completely suppressed the transcriptional silencing of mini $\mu$ .ter310. Together with the ChIP data, this suggests that NMTGS is established through deacetylation of histones at the genomic loci where PTC<sup>+</sup> mini $\mu$  genes have been integrated, most likely by recruiting HDACs to these sites. Notably, tran-

scription of neomycin also increased 3-fold upon SB treatment and reached the level measured in PTC-free constructs (Table S1), supporting the idea that the transcriptional silencing is caused by chromatin remodeling that spreads to some extent beyond the mini $\mu$  genes, affecting also the neighboring neomycin genes.

In searching for an alternative experimental approach, we reasoned that if SB specifically affected transcription without influencing posttranscriptional processes, changes in transcription rates should result in corresponding changes in mRNA levels. Therefore, we treated cells with SB or with trichostatin A (TSA), another HDAC inhibitor, and determined relative mini $\mu$  mRNA levels by quantitative real-time RT-PCR. 18S rRNA served as an internal control for normalization. As shown in Figures 4B and 4C, the same cell pool used for the nuclear run-on analysis in Figure 4A showed a 12-fold increase of mini $\mu$  mRNA in response to SB and TSA, similar to the 8-fold increase observed by nuclear run-on. We conclude that the changes on mini $\mu$  transcription caused by histone hyperacetylation result in corresponding changes of mini $\mu$  mRNA levels and therefore decided to analyze the effect of SB treatment on expression of all other constructs by real-time RT-PCR. As illustrated in Figure 4B, the roughly 100-fold reduced mini $\mu$ .ter310 mRNA level (relative to mini $\mu$ .wt) results from the combination of an about 10-fold reduced transcription rate and an additional 10-fold post-transcriptional reduction by NMD.

In contrast to the 12-fold increase of mini $\mu$ .ter310 mRNA, all mRNA levels of PTC-free mini $\mu$  constructs did not change significantly (increase < 2-fold; Figure 4C), confirming the PTC specificity of NMTGS. As for mini $\mu$ .ter310, SB treatment of cells expressing mini $\mu$ .ter73 resulted in an increase of mini $\mu$  mRNA (5-fold; Figure 4D) that is similar to the 3.3-fold reduced transcription rate (Figure 2A), indicating that SB completely reversed NMTGS of mini $\mu$ .ter73. Notably, neomycin mRNA levels also increased after SB treatment of cells expressing PTC<sup>+</sup> mini $\mu$ , but not in cells expressing PTC-free mini $\mu$  (data not shown), further supporting the idea that the chromatin remodeling induced by PTCs in mini $\mu$  spreads to neighboring genes.

Importantly, the relative Ig- $\mu$  mRNA levels and their changes upon SB treatment are highly reproducible in different cell populations independently transfected with the same mini $\mu$  construct (Figure 4E), ruling out the possibility that different average transgene copy numbers or differences in genomic integration sites could account for the observed differences between PTC<sup>+</sup> and PTC-free mini $\mu$ -expressing cells. Furthermore, we determined the relative average number of integrated plasmids in each of the cell populations shown in Figure 4E by real-time PCR of genomic DNA and found no correlation between plasmid copy number and the extent of transcriptional silencing (Table S2).

### NMTGS Might Be Ig Specific

We next investigated whether PTCs in other genes also induced transcriptional gene silencing. To this end, we stably transfected HeLa cells with PTC<sup>+</sup> or PTC-free versions of three well-studied NMD reporter genes (TCR- $\beta$ ,  $\beta$ -globin, and GPx1) (Buhler et al., 2002; Carter

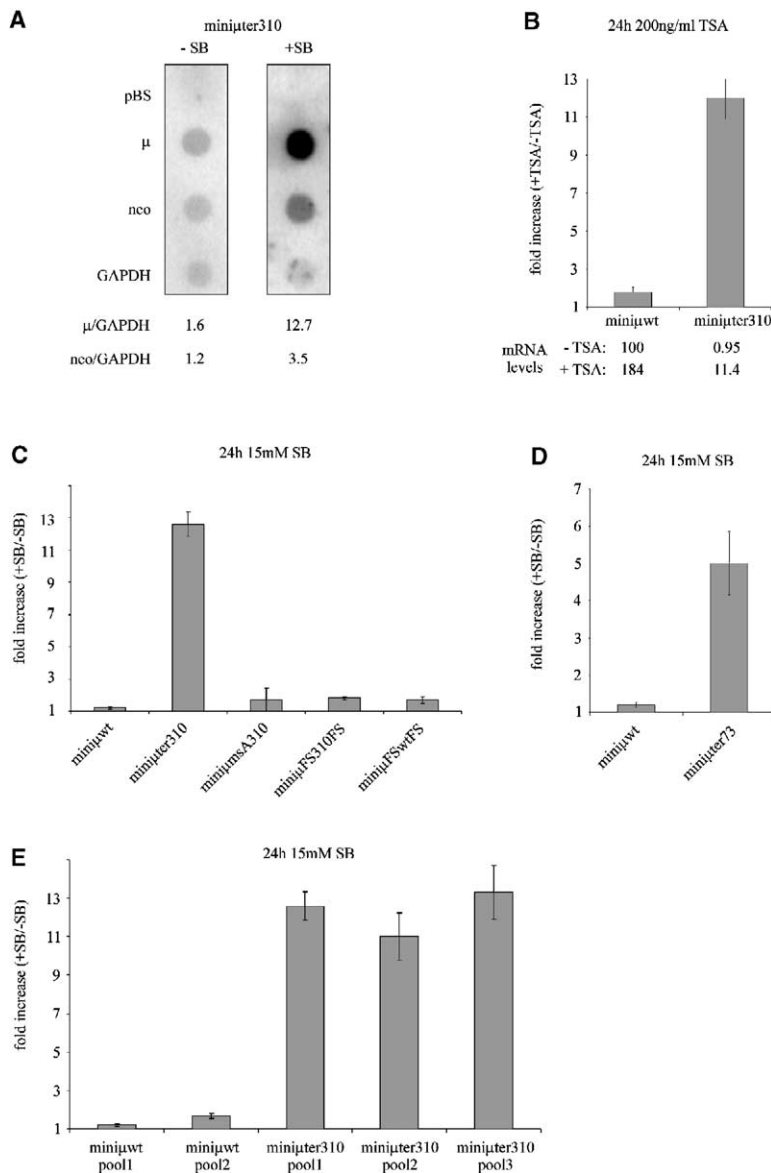


Figure 4. Histone Deacetylase Inhibitors Reverse the Transcriptional Silencing of PTC<sup>+</sup> Miniμ Genes

(A) Nuclear run-on assays performed with nuclei from HeLa cells expressing miniμter310 (same polyclonal cell pool as in Figure 2A) treated with 15 mM sodium butyrate for 24 hr (+SB). The signal intensity of each dot was quantified, and the values for miniμ and neomycin (neo) were normalized to GAPDH and are depicted below the filter strips (μ/GAPDH and neo/GAPDH, respectively). For comparison with the corresponding untreated sample, the same filter strip as in Figure 2A is shown for -SB.

(B-E) Cells expressing the indicated miniμ constructs were treated with 15 mM SB (C-E) or 200 ng/ml Trichostatin A (TSA; B) for 24 hr, and RNA was analyzed by real-time RT-PCR. Relative miniμ mRNA levels were determined and normalized to 18S rRNA, which served as internal control. The ratio of treated/untreated cells is shown as fold increase. (E) The increase of miniμter310 mRNA levels upon SB treatment is highly reproducible in three independently transfected polyclonal cell pools, whereas no significant increase (<2-fold) is observed in two independent cell pools expressing miniμwt. (B-E) Average values and SDs of three real-time PCR runs of one typical experiment are shown.

et al., 1996; Moriarty et al., 1997; Muhlemann et al., 2001; Thermann et al., 1998) and generated polyclonal cell pools as described for miniμ. These cells were then treated with SB, and mRNA levels were determined by real-time RT-PCR. In contrast to miniμ, none of these genes showed upregulation of PTC<sup>+</sup> mRNA levels after SB treatment (Figures 5A-5C).

Transcription of the β-globin constructs, which are under control of the β-globin promoter, was boosted by SB about 10-fold, irrespective of whether a PTC was present or not (Figure 5A), indicating that these transgenes assemble into heterochromatin in HeLa cells like the endogenous β-globin locus (Kim and Dean, 2004). Similarly, expression of the CMV promoter-driven GPx1 genes was increased about 4-fold upon SB treatment but independent of the presence or absence of a PTC (Figure 5B). The TCR-β minigenes used in Figure 5C were expressed from the same plasmid vector as the

miniμ genes in which the human β-actin promoter controls transcription of the inserted minigenes. This promoter assembles a transcriptionally fully active chromatin structure that cannot be further activated by inhibition of HDACs, as judged from the unaltered mRNA levels of PTC-free Ig-μ and TCR-β minigenes (Figures 4 and 5C). In contrast to miniμ, PTCs in two different exons of TCR-β do not show any signs of NMTGS. Given the unorthodox effects of Ig-μ and TCR-β in response to PTCs (see Introduction), this result was unexpected. Importantly, this result shows that the NMTGS-inducing signal must reside in the transcribed part of the Ig-μ gene and therefore suggests that NMTGS may be gene specific. In addition, these results demonstrate that SB does not interfere with NMD.

To test the possibility that NMTGS might be specific for Ig genes, we constructed an Ig-γ minigene from sequences of a productively rearranged human γ-1 heavy

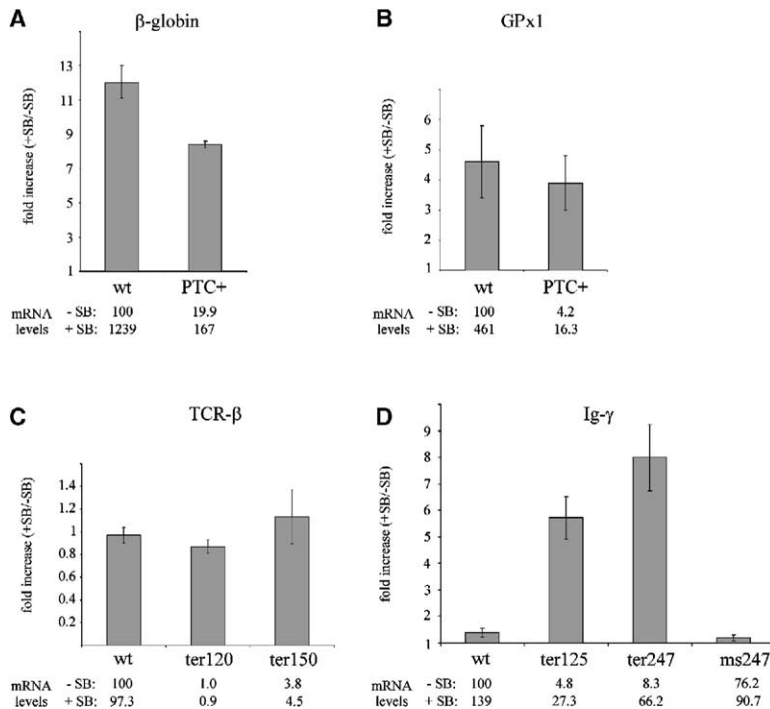


Figure 5. NMTGS May Be Ig Specific, and Sodium Butyrate Does Not Affect NMD

Well-studied NMD reporter constructs derived from  $\beta$ -globin, GPx1, and TCR- $\beta$ , and minigene constructs derived from a human Ig- $\gamma$  gene, were stably expressed in polyclonal cell populations exactly as described for mini- $\mu$  constructs. Cells were treated with 15 mM SB for 24 hr, and relative mRNA levels were measured by real-time RT-PCR as in Figure 4. Average mRNA levels (normalized to 18S rRNA and displayed relative to the corresponding wt mRNA level in untreated cells) of at least three real-time PCR runs of one typical experiment are shown below each panel. For each cell pool, the average mRNA ratio and SD of treated/untreated cells is shown as fold increase.

- (A) PTC+  $\beta$ -globin has a UAG codon at amino acid position 39.  
 (B) PTC+ GPx1 has a UAA codon at amino acid 46, whereas the wt construct has a UGC codon at this position.  
 (C) The PTC in TCR- $\beta$  ter120 is in the 3' part of the VDJ exon, and ter150 resides in exon C1.  
 (D) Ig- $\gamma$  ter125, ter247, and ms247 were derived from Ig- $\gamma$  wt by changing codon 125 from TTG to TAG, codon 247 from TGC to TGA, and to TTA, respectively.

chain (Persic et al., 1997). By site-directed point mutations, we inserted PTCs at two different positions, and stably expressed these constructs in HeLa cells, as described for the mini- $\mu$  constructs, by using the same expression vector. As shown in Figure 5D, treatment of the cells with SB increased the mRNA levels of the PTC+ Ig- $\gamma$  constructs 6- to 8-fold, whereas the mRNA levels of the PTC-free wt and ms247 constructs increased only marginally. Almost identical results were obtained when the cells were treated with TSA (data not shown). Because the ter247-generating point mutation (TGC to TGA, mutated nucleotide in bold) results in transcriptional silencing, whereas an additional point mutation (TGC to TTA) to generate ms247 does not, it strongly suggests that like Ig- $\mu$ , the transcriptional silencing of Ig- $\gamma$  minigenes is also PTC specific. The finding that PTCs in two different Ig genes caused transcriptional silencing, but not in three other genes, suggests that Ig genes might have evolved specific NMTGS-inducing cis-acting signals (see Discussion). More importantly, the results with the Ig- $\gamma$  minigenes demonstrate that NMTGS is not just an idiosyncrasy of our Ig- $\mu$  minigene system.

#### Is NMTGS Established via RNAi-Mediated Heterochromatin Assembly?

One of the most intriguing aspects of NMTGS is that a translation signal (i.e., a PTC) signals back information to its cognate gene to specifically repress its transcription. The trigger for NMTGS could be RNA, because it maps to the transcribed part of the mini- $\mu$  gene. Although RNA-based transcriptional gene silencing in plants is well documented (Baulcombe, 2004; Jorgensen, 2003; Matzke et al., 2001), it was only recently shown that in *S. pombe* and *D. melanogaster*, some

transcriptional silencing of genes by means of chromatin remodeling involves components of the RNA interference (RNAi) system and is triggered by small, double-stranded RNA molecules (Hall et al., 2002; Motamedi et al., 2004; Pal-Bhadra et al., 2004; Schramke and Allshire, 2003; Verdell et al., 2004; Volpe et al., 2002). During the last few months, evidence for RNAi-dependent transcriptional silencing in vertebrates has also been reported. It was demonstrated in chicken cells and mouse embryonic stem cells that Dicer is essential for formation of heterochromatin (Fukagawa et al., 2004; Kanellopoulou et al., 2005). Based on all these findings, it is tempting to speculate that similar small RNA molecules might trigger NMTGS. In particular, the association of NMTGS with K9 methylation of histone H3 is reminiscent of the siRNA-mediated heterochromatin assembly observed in centromeric regions of the *S. pombe* genome (Hall et al., 2002; Motamedi et al., 2004; Schramke and Allshire, 2003; Verdell et al., 2004; Volpe et al., 2002). To address this hypothesis, we sought for a way to interfere with RNAi and siRNA production in order to test if this affects NMTGS.

#### 3'hExo Inhibits RNAi

The protein 3'hExo was initially characterized as an exonuclease that binds to the hairpin at the 3' end of cell cycle-dependent histone mRNAs and is involved in their rapid degradation at the end of S phase (Dominski et al., 2003). However, recent data showed that it degrades double-stranded siRNAs in vitro and suggested that 3'hExo is the ortholog of the *C. elegans* siRNase ERI-1 (Kennedy et al., 2004). If 3'hExo indeed is an siRNase, its overexpression in human cells would be expected to inhibit RNAi. To test this, we knocked down a constitutively expressed reporter mRNA by express-

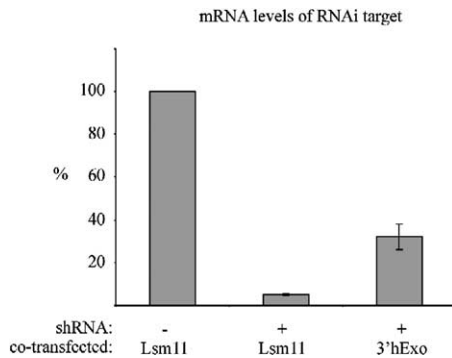


Figure 6. Overexpression of 3' hExo Inhibits RNAi

HeLa cells expressing a TCR- $\beta$  minigene were transfected with a pSUPERpuro plasmid encoding a shRNA targeting TCR- $\beta$  mRNA for degradation by RNAi (+) or with the empty pSUPERpuro as a control (-), together with a 3' hExo-encoding expression plasmid (3' hExo) or an identical expression plasmid encoding an unrelated protein (Lsm11). Relative TCR- $\beta$  mRNA levels were quantified by real-time RT-PCR 96 hr posttransfection and normalized to endogenous GAPDH mRNA levels. Average values and SDs of three real-time PCR runs are shown.

ing a short hairpin RNA (shRNA). When the shRNA-encoding plasmid was cotransfected with a plasmid expressing an unrelated control protein (Lsm11 [Pillai et al., 2003]), the mRNA level of the RNAi target was reduced to about 5% (Figure 6), and the same knockdown efficiency was achieved without cotransfection of Lsm11 (data not shown). In contrast, when the 3' hExo-expressing plasmid was cotransfected with the shRNA-encoding plasmid, the RNAi-mediated knockdown of the reporter mRNA was about 8-fold less efficient, providing in vivo evidence for the previously postulated function of 3' hExo as a siRNase (Figure 6).

#### Overexpression of the siRNase 3' hExo Suppresses NMTGS

After having found that overexpression of 3' hExo counteracts RNAi, we next wanted to test whether it also had an effect on NMTGS. To this end, we stably transfected recombinant 3' hExo together with either mini $\mu$ .wt or mini $\mu$ .ter310 and selected polyclonal cell populations. As a control, we cotransfected together with either mini $\mu$ .wt or mini $\mu$ .ter310 the unrelated protein Lsm11, driven by the same strong viral promoter (CMV) as 3' hExo. Relative mini $\mu$  pre-mRNA levels were then measured by real-time RT-PCR. As shown in Figure 7A, neither Lsm11 nor 3' hExo overexpression influenced mini $\mu$ .wt pre-mRNA levels. In contrast, 14-fold more mini $\mu$ .ter310 pre-mRNA was measured in 3' hExo-expressing cells compared to Lsm11-expressing cells (Figure 7B), demonstrating that overexpression of 3' hExo strongly inhibits NMTGS. We conclude that NMTGS was completely suppressed in this experiment, because SB treatment of the 3' hExo-expressing cells did not further increase mini $\mu$ .ter310 pre-mRNA levels, and because the 14-fold higher pre-mRNA level is very similar to the previously observed increase of mini $\mu$ .ter310 mRNA upon SB or TSA treatment (Figure 4). In light of the in vitro (Kennedy et al., 2004) and in vivo

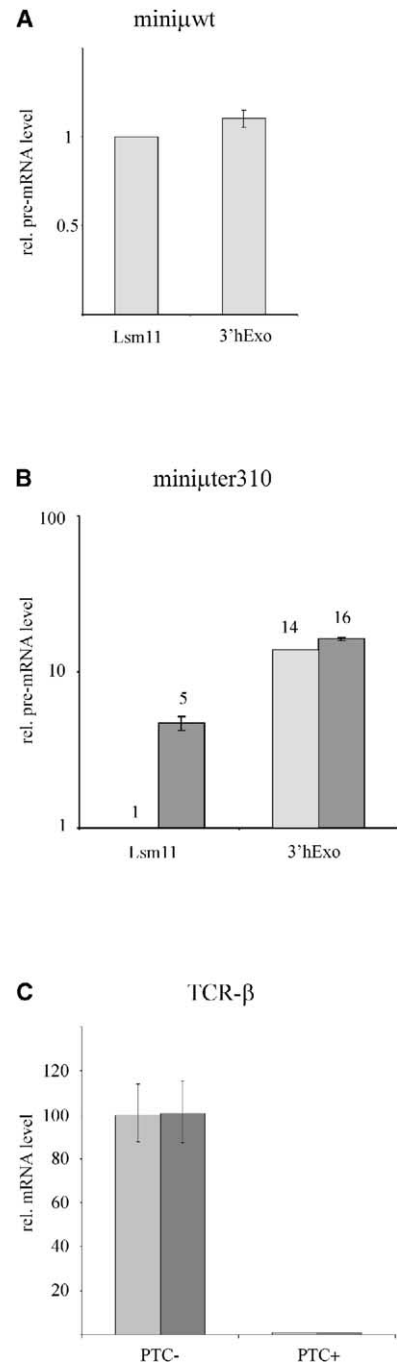


Figure 7. Overexpression of 3' hExo Inhibits NMTGS, but Not NMD (A and B) HeLa cells were stably cotransfected with mini $\mu$ .wt (A) or mini $\mu$ .ter310 (B) together with either Lsm11 or 3' hExo. Relative mini $\mu$  pre-mRNA levels were quantified by real-time RT-PCR and normalized to endogenous 18S rRNA. (B) Dark gray bars: cells were treated with 15 mM SB for 24 hr before RNA analysis. (C) Polyclonal HeLa cells stably expressing a PTC-free TCR- $\beta$  construct (PTC<sup>-</sup>) or the same TCR- $\beta$  gene with a PTC at amino acid 120 (PTC<sup>+</sup>) (Buhler et al., 2002; Muhlemann et al., 2001) were transfected with either Lsm11 (light gray bars) or 3' hExo (dark gray bars). Relative TCR- $\beta$  mRNA levels were analyzed by real-time RT-PCR 48 hr posttransfection and normalized to endogenous GAPDH mRNA levels. Average values and SDs of three real-time PCR runs of one typical experiment are shown.

(Figure 6) evidence for 3'hExo being a siRNase, this finding strongly suggests that small siRNA-like molecules are involved in NMTGS. However, our attempts to detect such proposed  $\mu$ -specific siRNA molecules were not successful so far (see Discussion).

### Overexpression of 3'hExo Does Not Interfere with NMD

As an additional control, we wanted to test if NMD was influenced in 3'hExo-overexpressing cells. HeLa cell lines stably expressing a PTC-free or a PTC<sup>+</sup> TCR- $\beta$  minigene (Muhlemann et al., 2001) were transfected with the 3'hExo-encoding expression vector or Lsm11 as a control, and relative TCR- $\beta$  mRNA levels were determined by real-time RT-PCR 48 hr posttransfection (Figure 7C). As expected, no change in the PTC<sup>+</sup> TCR- $\beta$  mRNA level was observed when 3'hExo was overexpressed, demonstrating that 3'hExo does not interfere with NMD. This result confirms that the restored mini $\mu$  pre-mRNA levels observed in Figure 7B are caused by inhibition of NMTGS and not by a direct effect of 3'hExo overexpression on NMD.

### Discussion

Collectively, our data reveal a hitherto undetected mechanism for controlling the quality of gene expression by showing that PTCs in Ig- $\mu$  minigenes lead to a transcriptional silencing of these genes. We demonstrate that this reduction of the transcription rate is specific for PTC-containing mini $\mu$ , because a corresponding missense mutation or additional frameshift mutations that restore the ORF by shifting the nonsense mutation out of frame did not lead to reduced transcription rates. The finding that the premature termination of the ORF appears to trigger the transcriptional silencing implicates that NMTGS depends on translation of the PTC<sup>+</sup> transcript and that it may be mechanistically linked to NMD. These predictions will be addressed in our future experiments. Unfortunately, the most direct way of testing whether NMTGS depends on NMD, namely knocking down essential NMD factors by RNAi, is not feasible for technical reasons. NMTGS takes about two weeks to fully establish after finishing the selection of the stably transfected cells (data not shown). In contrast, human cells in which the NMD factors hUpf1 or hSmg6 are depleted/reduced by RNAi die one week after induction of RNAi (A. Paillusson and O.M., unpublished data). Formally, NMTGS could also function entirely independent of NMD but that would imply the existence of a second, yet undiscovered cellular mechanism with the capability of recognizing PTCs. That PTCs in positions where they normally do not elicit NMD still result in 3- to 5-fold reduced mini $\mu$  mRNA levels (Buhler et al., 2004) would be consistent with a NMD-independent mechanism of PTC recognition. However, more work is required to determine if this mRNA reduction results from reduced transcription (i.e., NMTGS) or from a special mode of NMD.

Although the 3'hExo overexpression experiment strongly suggests the existence of a siRNA-like molecule that is involved in inducing NMTGS, we have so far not been able to detect a  $\mu$ -specific small RNA. Although the reason for our failure to detect the proposed

siRNAs might be technical, it is also possible that this putative siRNA is only required during an initial short window of time to establish NMTGS. Once established, the transcriptionally silent chromatin state might maintain itself by the presence of histone methyltransferases bound to the chromatin. If this scenario was true, we might have missed the peak of siRNA production in our experiments. Consistent with this possibility, 3'hExo overexpression only suppressed NMTGS when 3'hExo was cotransfected and stably expressed together with mini $\mu$ , but not when it was transiently overexpressed for 48 hr in cells where NMTGS was already established (data not shown).

An important question is how this putative siRNA would be generated in a PTC-specific manner. Among the different possibilities, we favor the idea that the putative siRNA is produced by Dicer during PTC recognition from a double-stranded portion of the PTC<sup>+</sup> transcript. Such a double-stranded RNA structure formed within the mini $\mu$  transcript would have to meet a number of criteria to be a substrate for Dicer, which could explain why NMTGS would only occur on a few specific genes that have evolved such secondary structures. Bioinformatics approaches to predict secondary structures in mini $\mu$  that might be Dicer substrates are underway, and future experiments will test the predicted requirement of Dicer for NMTGS. In one variant of this working model, the substrate for Dicer would be a degradation intermediate from NMD, and PTC specificity would be achieved simply because of the high degradation rate of PTC<sup>+</sup> transcripts, resulting in accumulation of enough siRNA molecules to induce NMTGS, whereas the slower turnover of PTC-free transcripts results in too little siRNA to trigger NMTGS. In another variant of this model, the NMD-associated RNA degradation might differ mechanistically and/or in its subcellular localization from normal degradation of PTC-free mRNAs, and these differences could restrict siRNA production to PTC<sup>+</sup> transcripts.

An alternative to a secondary structure in the mRNA being the trigger for NMTGS would be that premature translation termination on Ig mRNAs might recruit a RNA-dependent RNA polymerase (RdRP) that converts the mRNA into a dsRNA and therewith induces the RNAi-dependent gene silencing in the same manner as sense cosuppression is believed to work in plants (Jorgensen, 2003). The caveat for this model is that the human genome does not appear to contain any genes with significant homology to the RdRPs of plants, fungi, and *C. elegans*, although RdRP activity has been detected in murine erythroleukemia cells (Volloch et al., 1987).

In this study, we further demonstrated that NMTGS is accompanied by a change in the posttranslational modifications of histone H3, indicative for chromatin remodeling from an open, hyperacetylated, and transcriptionally active state to a condensed, transcriptionally inactive state. K9 methylation of histone H3, the modification enriched at PTC<sup>+</sup> mini $\mu$  loci, has been reported to be associated with transcriptionally silent heterochromatin (Litt et al., 2001; Nakayama et al., 2001; Noma et al., 2001). It will be interesting to find out if in addition to the monomethylated K9-H3, dimethylated K9-H3 is also associated with PTC<sup>+</sup> mini $\mu$ . Mono- and dimethylated K9-H3 has been specifically localized

to transcriptionally silent domains within euchromatin (so-called facultative heterochromatin), whereas trimethylated K9-H3 is enriched in pericentric regions of constitutive heterochromatin (Peters et al., 2003; Rice et al., 2003).

To the best of our knowledge, our results represent the first observation of PTCs affecting gene expression on the transcriptional level. Notably, reduced transcription rates of PTC<sup>+</sup> Ig- $\mu$  genes were not observed previously with different experimental systems (Jack et al., 1989; Muhlemann et al., 2001). To investigate the physiological relevance of NMTGS, B cell lines that contain a nonproductively (i.e., PTC<sup>+</sup>) and a productively rearranged heavy chain allele need to be generated and studied. We hypothesize that NMTGS in combination with NMD may be important for correct antibody production in B cells by ensuring that nonproductively rearranged alleles are kept silent. Such a combined transcriptional and posttranscriptional nonsense surveillance system would provide an elegant solution for the immune system to efficiently prevent the production of C-terminally truncated heavy chains, which if synthesized would be expected to seriously interfere with proper antibody production.

Finally, our results, together with other very recent publications (Fukagawa et al., 2004; Kanellopoulou et al., 2005), show that RNAi-mediated transcriptional gene silencing is not only restricted to invertebrates but also exists in mammals. In the examples reported so far, RNAi-mediated transcriptional silencing is triggered by aberrant, noncoding RNA transcripts. In a broader sense, PTC<sup>+</sup> mRNAs are also aberrant transcripts, and common cues might therefore exist that mark transcripts as “aberrant” and trigger transcriptional silencing. Notably, *C. elegans* strains with mutations in three of the seven known NMD factors have a defect in the persistence of RNAi, but the underlying mechanism of this genetic link between NMD and RNAi is not known (Domeier et al., 2000). Clearly, more work is required to better understand how transcripts are recognized as aberrant and how RNAi functions in promoting chromatin remodeling to transcriptionally silence the loci from which the aberrant transcripts originate.

## Experimental Procedures

### Plasmids and Cell Lines

The Ig- $\gamma$ 1 gene from pVHExpress 22/5 (Persic et al., 1997) was inserted into KpnI-BamHI of p $\beta$ 510 (Paillusson et al., 2005). In this expression vector, the Ig- $\mu$  and Ig- $\gamma$  minigenes are under the control of the human  $\beta$ -actin promoter. Nonsense, missense, and frameshift mutations creating Ig $\gamma$ ter125, Ig $\gamma$ ter247, Ig $\gamma$ ms247, mini $\mu$ FSwtFS, mini $\mu$ FS310FS, and mini $\mu$ msA310 were generated by site-directed mutagenesis using the QuikChange XL Site-Directed Mutagenesis Kit or the QuikChange Multi Site-Directed Mutagenesis Kit (Stratagene). Sequences of the mutagenic primers are available on request. The sequence of the entire ORF in each construct was confirmed by sequencing. All other mini $\mu$ ,  $\beta$ -globin, TCR- $\beta$ , and GPx1 constructs are described elsewhere (Buhler et al., 2002; Buhler et al., 2004; Carter et al., 1996; Moriarty et al., 1997; Muhlemann et al., 2001; Thermann et al., 1998). The ORF of 3' hExo (Dominski et al., 2003) was inserted EcoRV-XbaI into pcDNA3 (Invitrogen). pcDNA3-Lsm11 is described elsewhere (Pillai et al., 2003). HeLa cells were transfected with lipofectamine (Invitrogen) according to the manufacturer's protocol, and polyclonal populations of stably transfected HeLa cells were obtained by selection with 0.5–1.0 mg/ml G418 (Roche) for 10–14 days. Prior to analysis, the cells were cultured in nonselective medium for at least 2 weeks.

### Nuclear Run-On Analysis

Nuclei were isolated as described previously (Buhler et al., 2002) and stored in 40% glycerol, 5 mM MgCl<sub>2</sub>, 100 nM EDTA, 2.5 mM TrisHCl (pH 8.25), 5 mM DTT, and 0.4 U RNasin (Promega) in liquid nitrogen. Per run-on,  $\sim 10^7$  nuclei were incubated with 11 MBq  $\alpha^{32}$ P-UTP (0.834  $\mu$ M), 0.5 mM ATP, 0.5 mM GTP, 0.5 mM CTP, 120 mM KCl, and 2.5 mM Mg-acetate for 30 min at 30°C. Subsequently, total RNA was isolated by using the Absolutely RNA RT-PCR Mini-prep Kit (Stratagene) and hybridized to a nylon filter on which 5  $\mu$ g of single-stranded DNA probe had been immobilized per dot. Single-stranded DNA was isolated from *E. coli* transformed with pBS KS(-) (Stratagene) containing antisense mini $\mu$ wt, neo, or GAPDH sequences and infected with helper phage M13K07 (New England Biolabs). Hybridization conditions were 24–30 hr at 60°C in 6 $\times$  SSC, 5 $\times$  Denhardt's, 0.5% SDS, 20 ng/ $\mu$ l denatured herring sperm DNA, and 100 ng/ $\mu$ l *E. coli* tRNA. Subsequently, filter strips were washed twice in 0.5  $\times$  SSC/0.1% SDS at 65°C for 15 min. Signals were visualized and quantified by PhosphorImager scanning. The signal of empty pBS on each filter was considered background and subtracted from the signals of the other dots.

### ChIP

ChIP was performed from formaldehyde-fixed, stably transfected HeLa cells by using the Acetyl-Histone H3 Immunoprecipitation (ChIP) Assay Kit (Upstate, 17-245) according to the manufacturer's protocol. 10  $\mu$ g  $\alpha$ -monomethyl-histone H3 (Lys9) antibody (Upstate, 05-713) was used to precipitate meK9-H3 using the same kit. Precipitated DNA fragments were quantified by real-time PCR (ABI SDS7000 Sequence Detection System) with specific primers and TaqMan probes (sequences available upon request) and normalized to endogenous 18S rDNA (acetyl-H3 ChIP) or endogenous  $\beta$ -globin DNA (meK9-H3 ChIP). 40 ng of control input DNA and 100 ng of immunoprecipitated DNA was amplified, respectively.

### Inhibition of HDACs and Quantitative RT-PCR

$3 \times 10^5$  cells were seeded in 6-well plates and treated the next day with 15 mM SB (Upstate) or 200 ng/ml TSA (Sigma) for 24 hr. Subsequently, total RNA was isolated as described above and 1  $\mu$ g RNA was reverse transcribed in 50  $\mu$ l Stratascript first strand buffer in the presence of 0.4 mM dNTPs, 300 ng random hexamers, 40 U RNasin (Promega), and 50 U Stratascript reverse transcriptase (Stratagene). For real-time PCR, reverse-transcribed material corresponding to 40 ng RNA was amplified in 25  $\mu$ l Universal PCR Master Mix, No AmpErase UNG (Applied Biosystems) with specific primers, and TaqMan probes (sequences are available upon request) by using the ABI SDS7000 Sequence Detection System.

### RNAi

RNAi of a TCR- $\beta$  minigene mRNA stably expressed in HeLa cells was induced by transfection of a puromycin-resistant pSUPER vector (Brummelkamp et al., 2002) targeting the sequence 5'-GGCTG ATCCATTACTCATA-3', and 24 hr after transfection, untransfected cells were eliminated by culturing the cells in the presence of 1.5  $\mu$ g/ml puromycin for 48 hr. Lsm11- or 3' hExo-encoding plasmids were cotransfected in 7-fold molar excess over the pSUPER-TCR $\beta$  plasmid. Total RNA was isolated 96 hr posttransfection. Conditions for reverse transcription and real-time PCR were as described above, using primers and a TaqMan probe specific for TCR- $\beta$  mRNA (Buhler et al., 2002).

### Supplemental Data

Supplemental data include Experimental Procedures, one figure, and two tables and are available online with this article at <http://www.molecule.org/cgi/content/full/18/3/307/DC1/>.

### Acknowledgments

We thank Karin Schranz for help with cell cultures; Monique Vogel for the Ig- $\gamma$  plasmid; and Witold Filipowicz, Dirk Schübeler, Beat Suter, and Daniel Schümperli for critical comments and suggestions. This work was supported by the Kanton Bern and grants to O.M. from the Swiss National Foundation, the Novartis Foundation for Biomedical Research, and the Helmut Horten Foundation.

Received: August 2, 2004  
Revised: March 17, 2005  
Accepted: March 31, 2005  
Published: April 28, 2005

## References

- Baulcombe, D. (2004). RNA silencing in plants. *Nature* 431, 356–363.
- Baumann, B., Potash, M.J., and Kohler, G. (1985). Consequences of frameshift mutations at the immunoglobulin heavy chain locus of the mouse. *EMBO J.* 4, 351–359.
- Brummelkamp, T.R., Bernards, R., and Agami, R. (2002). A system for stable expression of short interfering RNAs in mammalian cells. *Science* 296, 550–553.
- Buhler, M., Wilkinson, M.F., and Muhlemann, O. (2002). Intranuclear degradation of nonsense codon-containing mRNA. *EMBO Rep.* 3, 646–651.
- Buhler, M., Paillusson, A., and Muhlemann, O. (2004). Efficient downregulation of immunoglobulin mu mRNA with premature translation-termination codons requires the 5'-half of the VDJ exon. *Nucleic Acids Res.* 32, 3304–3315.
- Carter, M.S., Li, S., and Wilkinson, M.F. (1996). A splicing-dependent regulatory mechanism that detects translation signals. *EMBO J.* 15, 5965–5975.
- Dillon, N., and Festenstein, R. (2002). Unravelling heterochromatin: competition between positive and negative factors regulates accessibility. *Trends Genet.* 18, 252–258.
- Domeier, M.E., Morse, D.P., Knight, S.W., Portereiko, M., Bass, B.L., and Mango, S.E. (2000). A link between RNA interference and nonsense-mediated decay in *Caenorhabditis elegans*. *Science* 289, 1928–1931.
- Dominski, Z., Yang, X.C., Kaygun, H., Dadlez, M., and Marzluff, W.F. (2003). A 3' exonuclease that specifically interacts with the 3' end of histone mRNA. *Mol. Cell* 12, 295–305.
- Fischle, W., Wang, Y., and Allis, C.D. (2003). Histone and chromatin cross-talk. *Curr. Opin. Cell Biol.* 15, 172–183.
- Fukagawa, T., Nogami, M., Yoshikawa, M., Ikeno, M., Okazaki, T., Takami, Y., Nakayama, T., and Oshimura, M. (2004). Dicer is essential for formation of the heterochromatin structure in vertebrate cells. *Nat. Cell Biol.* 6, 784–791.
- Gatfield, D., and Izaurralde, E. (2004). Nonsense-mediated messenger RNA decay is initiated by endonucleolytic cleavage in *Drosophila*. *Nature* 429, 575–578.
- Gatfield, D., Unterholzner, L., Ciccarelli, F.D., Bork, P., and Izaurralde, E. (2003). Nonsense-mediated mRNA decay in *Drosophila*: at the intersection of the yeast and mammalian pathways. *EMBO J.* 22, 3960–3970.
- Gudikote, J.P., and Wilkinson, M.F. (2002). T-cell receptor sequences that elicit strong down-regulation of premature termination codon-bearing transcripts. *EMBO J.* 21, 125–134.
- Hall, I.M., Shankaranarayana, G.D., Noma, K., Ayoub, N., Cohen, A., and Grewal, S.I. (2002). Establishment and maintenance of a heterochromatin domain. *Science* 297, 2232–2237.
- Jack, H.M., Berg, J., and Wabl, M. (1989). Translation affects immunoglobulin mRNA stability. *Eur. J. Immunol.* 19, 843–847.
- Jenuwein, T., and Allis, C.D. (2001). Translating the histone code. *Science* 293, 1074–1080.
- Jorgensen, R.A. (2003). Sense cosuppression in plants: past, present, and future. In *RNAi: A Guide to Gene Silencing*, G.J. Hannon, ed. (Cold Spring Harbor, NY: Cold Spring Harbor Laboratory Press), pp. 5–21.
- Jung, D., and Alt, F.W. (2004). Unraveling V(D)J recombination; insights into gene regulation. *Cell* 116, 299–311.
- Kanellopoulou, C., Muljo, S.A., Kung, A.L., Ganesan, S., Drapkin, R., Jenuwein, T., Livingston, D.M., and Rajewsky, K. (2005). Dicer-deficient mouse embryonic stem cells are defective in differentiation and centromeric silencing. *Genes Dev.* 19, 489–501.
- Kennedy, S., Wang, D., and Ruvkun, G. (2004). A conserved siRNA-degrading RNase negatively regulates RNA interference in *C. elegans*. *Nature* 427, 645–649.
- Kim, A., and Dean, A. (2004). Developmental stage differences in chromatin subdomains of the beta-globin locus. *Proc. Natl. Acad. Sci. USA* 101, 7028–7033.
- Li, S., and Wilkinson, M.F. (1998). Nonsense surveillance in lymphocytes? *Immunity* 8, 135–141.
- Litt, M.D., Simpson, M., Gaszner, M., Allis, C.D., and Felsenfeld, G. (2001). Correlation between histone lysine methylation and developmental changes at the chicken beta-globin locus. *Science* 293, 2453–2455.
- Maquat, L.E. (2004). Nonsense-mediated mRNA decay: splicing, translation and mRNP dynamics. *Nat. Rev. Mol. Cell Biol.* 5, 89–99.
- Matzke, M.A., and Birchler, J.A. (2005). RNAi-mediated pathways in the nucleus. *Nat. Rev. Genet.* 6, 24–35.
- Matzke, M.A., Matzke, A.J.M., Pruss, G.J., and Vance, V.B. (2001). RNA-based silencing strategies in plants. *Curr. Opin. Genet. Dev.* 11, 221–227.
- Mendell, J.T., and Dietz, H.C. (2001). When the message goes awry: disease-producing mutations that influence mRNA content and performance. *Cell* 107, 411–414.
- Moriarty, P.M., Reddy, C.C., and Maquat, L.E. (1997). The presence of an intron within the rat gene for selenium-dependent glutathione peroxidase 1 is not required to protect nuclear RNA from UGA-mediated decay. *RNA* 3, 1369–1373.
- Motamedi, M.R., Verdell, A., Colmenares, S.U., Gerber, S.A., Gygi, S.P., and Moazed, D. (2004). Two RNAi complexes, RITS and RDRC, physically interact and localize to noncoding centromeric RNAs. *Cell* 119, 789–802.
- Muhlemann, O., Mock-Casagrande, C.S., Wang, J., Li, S., Custodio, N., Carmo-Fonseca, M., Wilkinson, M.F., and Moore, M.J. (2001). Precursor RNAs harboring nonsense codons accumulate near the site of transcription. *Mol. Cell* 8, 33–43.
- Nagy, E., and Maquat, L.E. (1998). A rule for termination-codon position within intron-containing genes: when nonsense affects RNA abundance. *Trends Biochem. Sci.* 23, 198–199.
- Nakayama, J., Rice, J.C., Strahl, B.D., Allis, C.D., and Grewal, S.I. (2001). Role of histone H3 lysine 9 methylation in epigenetic control of heterochromatin assembly. *Science* 292, 110–113.
- Noma, K., Allis, C.D., and Grewal, S.I. (2001). Transitions in distinct histone H3 methylation patterns at the heterochromatin domain boundaries. *Science* 293, 1150–1155.
- Ochi, A., Hawley, R.G., Hawley, T., Shulman, M.J., Traunecker, A., Kohler, G., and Hozumi, N. (1983). Functional immunoglobulin M production after transfection of cloned immunoglobulin heavy and light chain genes into lymphoid cells. *Proc. Natl. Acad. Sci. USA* 80, 6351–6355.
- Paillusson, A., Hirschi, N., Vallan, C., Azzalin, C.M., and Muhlemann, O. (2005). A GFP-based reporter system to monitor nonsense-mediated mRNA decay. *Nucleic Acids Res.* 33, e54.
- Pal-Bhadra, M., Leibovitch, B.A., Gandhi, S.G., Rao, M., Bhadra, U., Birchler, J.A., and Elgin, S.C. (2004). Heterochromatic silencing and HP1 localization in *Drosophila* are dependent on the RNAi machinery. *Science* 303, 669–672.
- Persic, L., Roberts, A., Wilton, J., Cattaneo, A., Bradbury, A., and Hoogenboom, H.R. (1997). An integrated vector system for the eukaryotic expression of antibodies or their fragments after selection from phage display libraries. *Gene* 187, 9–18.
- Peters, A.H., Kubicek, S., Mechtler, K., O'Sullivan, R.J., Derijck, A.A., Perez-Burgos, L., Kohlmaier, A., Opravil, S., Tachibana, M., Shinkai, Y., et al. (2003). Partitioning and plasticity of repressive histone methylation states in mammalian chromatin. *Mol. Cell* 12, 1577–1589.
- Pillai, R.S., Grimmmer, M., Meister, G., Will, C.L., Luhrmann, R., Fischer, U., and Schumperli, D. (2003). Unique Sm core structure of U7 snRNPs: assembly by a specialized SMN complex and the role of a new component, Lsm11, in histone RNA processing. *Genes Dev.* 17, 2321–2333.
- Rice, J.C., Briggs, S.D., Ueberheide, B., Barber, C.M., Shabanowitz,

- J., Hunt, D.F., Shinkai, Y., and Allis, C.D. (2003). Histone methyltransferases direct different degrees of methylation to define distinct chromatin domains. *Mol. Cell* *12*, 1591–1598.
- Schramke, V., and Allshire, R. (2003). Hairpin RNAs and retrotransposon LTRs effect RNAi and chromatin-based gene silencing. *Science* *301*, 1069–1074.
- Singh, G., and Lykke-Andersen, J. (2003). New insights into the formation of active nonsense-mediated decay complexes. *Trends Biochem. Sci.* *28*, 464–466.
- Thermann, R., Neu-Yilik, G., Deters, A., Frede, U., Wehr, K., Hagemeyer, C., Hentze, M.W., and Kulozik, A.E. (1998). Binary specification of nonsense codons by splicing and cytoplasmic translation. *EMBO J.* *17*, 3484–3494.
- Verdel, A., Jia, S., Gerber, S., Sugiyama, T., Gygi, S., Grewal, S.I., and Moazed, D. (2004). RNAi-mediated targeting of heterochromatin by the RITS complex. *Science* *303*, 672–676.
- Volloch, V., Schweitzer, B., and Rits, S. (1987). Synthesis of globin RNA in enucleated differentiating murine erythroleukemia cells. *J. Cell Biol.* *105*, 137–143.
- Volpe, T.A., Kidner, C., Hall, I.M., Teng, G., Grewal, S.I., and Martienssen, R.A. (2002). Regulation of heterochromatic silencing and histone H3 lysine-9 methylation by RNAi. *Science* *297*, 1833–1837.
- Wang, J., Gudikote, J.P., Olivas, O.R., and Wilkinson, M.F. (2002). Boundary-independent polar nonsense-mediated decay. *EMBO Rep.* *15*, 274–279.
- Wilusz, C.J., Wang, W., and Peltz, S.W. (2001). Curbing the nonsense: the activation and regulation of mRNA surveillance. *Genes Dev.* *15*, 2781–2785.